

CARBONATE FORMATION IN GLEN TORRIDON, GALE CRATER, MARS. S. M. R. Turner¹, S. P. Schwenzer¹, J. C. Bridges², B. Sutter³, M.T. Thorpe³, E.B. Rampe⁴, and A.C. McAdam⁵. ¹AstrobiologyOU, STEM Faculty, The Open University, UK, (stuart.turner@open.ac.uk). ²School of Physics and Astronomy, University of Leicester, UK. ³Jacobs, NASA JSC, USA. ⁴NASA JSC, USA. ⁵NASA Goddard Space Flight Center, USA.

Introduction: Identification of martian carbonate and understanding its formation are important in Mars geochemistry studies. It offers a way to track changes in atmosphere-water-crust interactions in the martian geological record [1]. The sediments of Glen Torridon (GT) in Gale crater were deposited in a predominantly lacustrine environment, and subsequently underwent multiple episodes of diagenesis [2-8]. Although traces of carbonate have been found by the SAM instrument throughout the Mars Science Laboratory mission, e.g., at Rocknest [9], Fe-carbonate has been detected with CheMin for the first time in the clay-rich GT region. Five out of seven drill samples from GT show Fe-carbonate alongside phyllosilicates [6]. Here we explore the possible reaction pathways of carbonate formation in GT and its associated fluid history (Fig. 1).

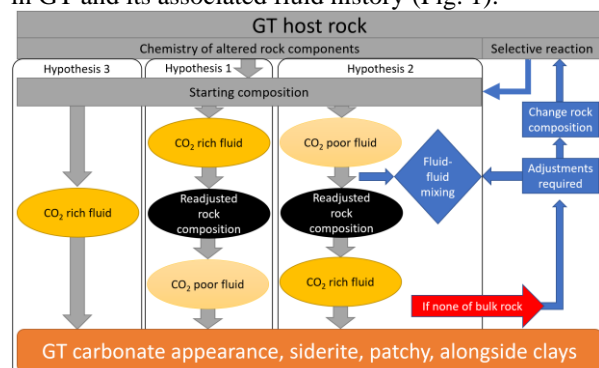


Fig. 1. Potential reaction pathways for modeling carbonate formation in Glen Torridon, Gale crater.

We have three hypotheses for the formation of the patchy carbonate occurrences within GT: (H1) Early carbonate formation with CO₂-rich fluids followed by a second alteration event with CO₂-poor fluids, (H2) low-CO₂ alteration followed by carbonate formation with CO₂-rich fluids, and (H3) direct formation by interaction with CO₂-rich fluids (Fig. 1). H1 tests early diagenetic carbonate formation followed by further alteration. Although geologic setting and temperature are different, this sequence of early carbonate formation followed by partial dissolution of the carbonate during clay formation has been observed in the nakhlites [10]. H2 tests a formation sequence of phyllosilicates followed by interaction of the altered rock with a CO₂-rich fluid. Fluid-fluid mixing was envisaged by [6], and percolating lake-water may have been the CO₂-rich fluid in our models.

Modeling Method: CHIM-XPT, a program for computing multicomponent heterogeneous chemical

equilibria in aqueous-mineral gas systems, calculates equilibrium for each water / rock reaction step between a user-defined fluid and dissolved chemical reactant list (the rock) [11] and has been used extensively in water-rock reaction studies for Gale [12-15]. Here we focus on 10-100,000 W/R, and the Holland and Powell (H&P) [16] and low-temperature BRGM Thermoddem [17] thermochemical databases were used.

The Starting Fluid. The model Gale groundwater, “Gale Portage Water” (GPW) [12], has previously been used in thermochemical modeling [13,14]. The solution is initially oxidizing, and Fe³⁺/Fe_{tot} ratio of the host rock controls the redox of the system throughout each model. Two HCO₃⁻ concentrations have been used, 1.68×10^{-4} and 5.24×10^{-2} moles/kg, from equilibration with an atmosphere of current (6 mbar) and Noachian/Early Hesperian Mars (~1 bar, see [18]) partial pressure (pCO₂), respectively.

The Reactant Rock. For the reactant rock composition, we used the summed chemistry of the alteration phases and amorphous component identified in the Kilmarie drill sample by APXS and CheMin, using the same methodology outlined in [14]. The Kilmarie drill sample, from the GT Jura member, was selected as it has minimal diagenetic overprint, with diagenetic features limited to cross-cutting Ca-sulfate veins [7] and minor amounts of general discoloration and pitting [8]. Mineralogically, CheMin analysis of Kilmarie shows 28 wt.% phyllosilicates, with 2.2 wt.% siderite, 1.1 wt.% hematite, and an amorphous content of 44 wt.% [6,19]. Ca-sulfates are also present but are attributed to a later phase of alteration than is of interest in this abstract [19]. CheMin and SAM analyses of the phyllosilicate are consistent with Fe³⁺-rich dioctahedral smectite. CheMin XRD also showed a low-angle peak at ~9.22 Å that may represent a mixed-layer serpentine-talc (2.8 wt.%), as supported by SAM EGA data [19].

Modeling Results: Here we show three models run at 50 °C (Fig. 2): two runs with CO₂-poor GPW using H&P and BRGM databases (Fig. 2a,b); and one run with CO₂-rich GPW using the BRGM database (Fig. 2c).

For the low-CO₂ GPW models, Fig. 2a,b show that at very high W/R ratios, oxides (goethite/hematite) dominate alongside sheet silicates. At low W/R the dominating sheet silicate for all models is serpentine. There are marked differences between the models calculated with the different databases in the phyllosilicates at high and medium W/R, though. For

the H&P database [16], nontronite is formed in the intermediate W/R, which is consistent with dioctahedral smectite observed by SAM in the Kilmarie drill sample [10]. Using the low-temperature specific BRGM database, a wider variety of clay minerals occurs. Fig. 2b. shows the dioctahedral smectite beidellite forming at high W/R, with the trioctahedral smectite saponite dominant over a wide W/R range. This is an important observation as it directly influences the Fe-balance on the remaining alteration mineralogy, forming more Fe-oxide in Fig. 2b compared to Fig. 2a.

Fig. 2c shows the interaction of CO₂-rich GPW with the calculated alteration chemistry of the Kilmarie drill sample. Beidellite forms over a greater W/R range than in Fig. 2b, with saponites being restricted to below 100 W/R in Fig. 2c compared to Fig. 2b. Greenalite in Fig. 2c forms at low W/R, similar to Fig. 2b. Hematite in Fig. 2c. is also restricted to lower W/R compared to Fig. 2b. From 20 to 3,333 W/R Fe-bearing carbonates siderite and ankerite form, with a peak abundance of 41.1 wt.% of the alteration phases at 500 W/R. Quartz forms from 20,000 W/R to 13 W/R in high abundance, which suggests cation unavailability in the fluid.

Discussion: Alteration of the Kilmarie-derived composition with CO₂-rich fluids (H1), shows the formation of siderite and ankerite over a wide range of W/R ratios (Fig. 2c). The abundance of quartz and phyllosilicate phases are not directly comparable to the observations made by *Curiosity*, suggesting further interaction with CO₂-poor fluids is required to produce widespread Fe³⁺-dioctahedral smectite coupled with patchy siderite as observed in GT. This also rules out a one-step GT alteration model (H3).

Whilst Fig. 2a,b suggest that carbonate formation within GT is not possible with a low concentration of CO₂ equivalent to equilibrium with current atmospheric pressure, further modelling will focus on the two-step H2. Thus, future models will include higher pCO₂ and/or a change in alteration conditions. In comparison, higher pCO₂ at ~150 °C was modeled for the initial carbonate formation in the nakhlite meteorites [10]. Given the abundance of Fe-oxides in Fig. 2, we assume that Fe-oxides are the dominant species throughout a wide range of CO₂-atmospheric/dissolved concentrations, especially as lower T increases the solubility of CO₂.

Summary: The models presented here point towards a two-step model for carbonate formation in GT. Siderite and ankerite shown in Fig 2c indicate that high pCO₂ is required, but the overall mineral assemblage argues against a one-step process. We are in the process of testing lower temperature regimes as well as fluid-fluid mixing scenarios to complete our two-step

models and determine which hypothesis, H1 or H2, is most representative of carbonate formation in GT.

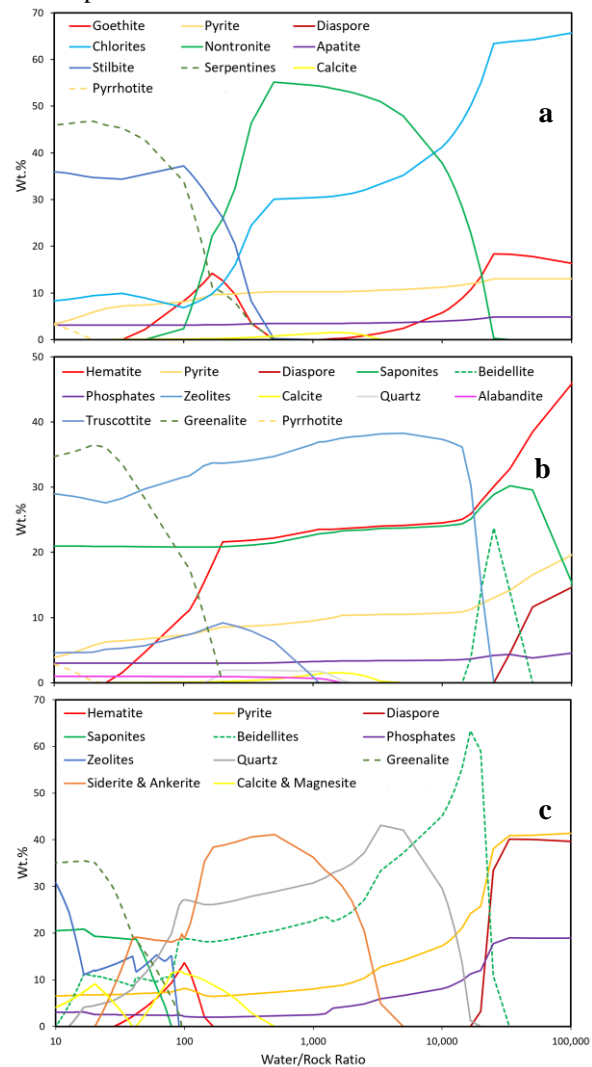


Fig. 2. CHIM-XPT model results from reacting the alteration chemistry of the Kilmarie drill sample, including 10 % Fe as Fe³⁺ of the host rock, with CO₂-poor GPW at 50 °C using the H&P database (a) and BRGM database (b), and with CO₂-rich GPW at 50 °C using the BRGM database (c).

References: [1] Bridges et al., 2019. Carbonates on Mars. In 'Volatiles on Mars'. 1st edition. Elsevier. [2] Grotzinger et al., 2015. *Science* 350(6257). [3] Fraeman et al., 2020. *JGR: Planets* 125(20), e2020JE006527. [4] Rampe et al., 2020. *Geochemistry* 80(2), 125605. [5] Rampe et al., 2020. *JGR: Planets* 125(12), e2019JE006306. [6] Thorpe et al., submitted. *JGR: Planets*. [7] Gasda et al., submitted. *JGR: Planets*. [8] Rudolph et al., submitted. *JGR: Planets*. [9] Archer Jr et al., 2014. *JGR: Planets* 119(1), 237-254. [10] Bridges and Schwenzer, 2012. *EPSL* 359, 117-123. [11] Reed 1998. *Rev. Econ Geol.* 10, 109-124. [12] Bridges et al., 2015. *JGR: Planets* 120(1), 1-19. [13] Schwenzer et al., 2016. *MaPS* 51(11), 2175-2202. [14] Turner et al., 2021. *MaPS* 56(10), 1905-1932. [15] Schieber et al., 2017. *Sedimentology* 64(2), 311-358. [16] Holland and Powell, 2011. *Journal of metamorphic Geology* 29(3), 333-383. [17] Blanc et al., 2012. *Applied Geochemistry* 27(10), 2107-2116. [18] Craddock and Greeley, 2009. *Icarus* 204(2), 512-526. [19] Bristow et al., 2021. *Science* 373(6551).